CORROSION SCIENCE AND TECHNOLOGY, Vol.17, No.2(2018), pp.54~59
[Research Paper]
pISSN: 1598-6462 / eISSN: 2288-6524
DOI: https://doi.org/10.14773/cst.2018.17.2.54

The Effect of External DC Electric Field on the Atmospheric Corrosion Behaviour of Zinc under a Thin Electrolyte Layer

Qinqin Liang[1], YanYang[2], Junxi Zhang[2,†], Xujie Yuan[2], and Qimeng Chen[2]

[1]*Guangxi Power Grid Electric Power Research Institute, Nanning 530023, China*
[2]*Shanghai Key Laboratory of Material Protection and Advanced Material in Electric Power, Shanghai University of Electric Power, Shanghai 200090, China*

(Received November 14, 2018; Revised March 31, 2018; Accepted April 05, 2018)

The effect of external DC electric field on atmospheric corrosion behavior of zinc under a thin electrolyte layer (TEL) was investigated by measuring open circuit potential (OCP), cathodic polarization curve, and electrochemical impedance spectroscopy (EIS). Results of OCP vs. time curves indicated that the application of external DC electric field resulted in a negative shift of OCP of zinc. Results of cathodic polarization curves measurement and EIS measurement showed that the reduction current of oxygen increased while charge transfer resistance (R_{ct}) decreased under the external DC electric field. Variation of OCP negative shift, reduction current of oxygen, and R_{ct} increase with increasing of external DC electric field strength as well as the effect of external DC electric field on double-layer structure in the electrode/electrolyte interface and ions distribution in thin electrolyte layer were analyzed. All results showed that the external DC electric field could accelerate the corrosion of zinc under a thin electrolyte layer.

Keywords: *Zinc, Polarization, EIS, Atmosphere corrosion, External DC electric field*

1. Introduction

Power transmission towers are affected mainly by atmospheric corrosion since all of them are served in atmospheric environment. When the electricity system is working, Alternating Current (AC)/Direct Current (DC) interference from the high-voltage transmission lines can occur around the transmission tower. Presently, according to power maintenance records, some galvanized parts of power transmission tower near the transmission lines, have significantly higher corrosion rates than that of the other part, which suggests that the electric field might promote the atmospheric corrosion process of the metal. Therefore, it is significant to study the mechanism of the effect of electric field on metal.

Since the seventies of last century, a number of laboratory and field studies have focused on the influence of AC and DC induced voltage on the behavior of corrosion systems. Most of the literatures have been concerned with the influence of AC on soil and solutions systems [1-5]. It has been reported that AC/DC interference from high-voltage transmission lines, can result in serious corrosion problems for buried pipelines. It has been demonstrated that AC electric field behaves as a depolarizer, which can reduce both anodic and cathodic polarizations, degrade the electrochemical passivity, and enhance the corrosion rate of metal [3,6-8].

In atmospheric environments, corrosion proceeds under a thin electrolyte layer during wet- dry cycles. The corrosion rate of metals is affected mainly by the composition of the surface corrosion products and mass transfer process of oxygen under a thin electrolyte layers (TELs). Many investigations on galvanized steel under various conditions have been reported over past decades [9,10]. Guo investigated the effects of electric field on atmospheric corrosion behavior of PCB-Cu under TELs, and demonstrated that the electric field reduce the corrosion rate of PCB-Cu owing to the aggressive ions migrating out from the PCB-Cu electrode surface under the effect of the electric field [11]. However, there has been limited work to study the effect of the external electric field on the atmospheric corrosion of zinc.

In this work, the effect of DC electric field on the atmospheric corrosion behaviour of zinc under a 0.35 wt% NaCl TEL was investigated by open circuit potential measurements, cathodic polarization and electrochemical impedance spectroscopy (EIS) using a homemade thin layer electrochemical cell.

† Corresponding author: zhangjunxi@shiep.edu.cn

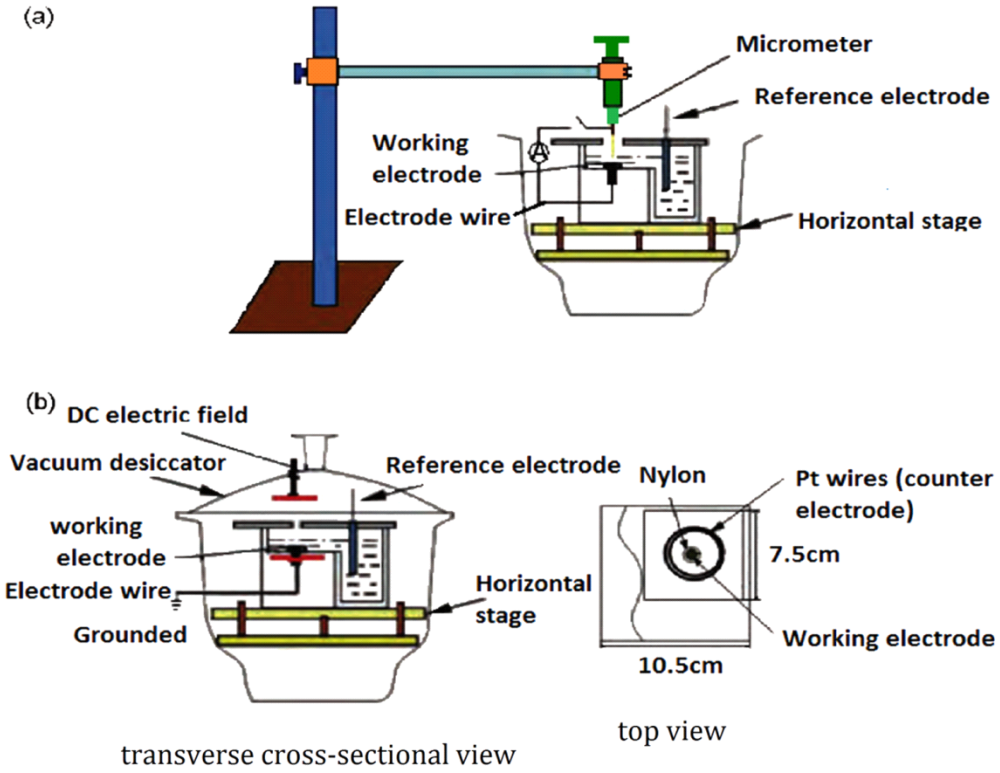

Fig. 1 (a) Schematic diagrams of the experimental arrangement for the TEL corrosion tests under a DC electric field, and (b) transverse cross-sectional and top views for the electrochemical cell.

2. Experimental

2.1 Materials and solution

The specimens used in the electrochemical measurement were pure zinc (99.95%) with a diameter of 10 mm. It is should be noted that the hot-dip galvanizing on the surface of carbon steel is different from that of metallic zinc. The zinc coating of hot-dip galvanizing contains multiple layers with different compositions, but the surface layer of the coating is similar to metallic zinc. For the convenience of study, and it is the initial corrosion behavior of atmospheric corrosion in this work. Therefore, zinc coating is replaced with pure zinc. The side surface of the electrode was sealed by nylon for better hydrophilic. The top cross-section was only exposed as working area. Before each experiment, the electrodes were polished through successive grades of silicon carbide abrasive papers from 500# to 2000#, degreased with acetone, washed with distilled water and dried with hair dryer. Then the electrodes were stored in moisture-free desiccators prior to use.

The electrolyte was 0.35 wt% NaCl solution, which was prepared from analytical grade reagent and distilled water. The device as showed in Fig. 1a for controlling the thin liquid film in this study consisted of a homemade micrometer, a platinum needle with a diameter of 0.5 mm, and an ohmmeter. The platinum needle was welded on the micrometer. TELs thickness measurement conducted before using a three-dimensional water platform to adjust the level. When the platinum needle touches the surface of the electrode without electrolyte, the ohmmeter will beep to record the scale position of the micrometer at this time. After the electrolyte is injected, when the platinum needle comes into contact with the TEL, there will be a noticeable arc fluctuation on the surface of the electrolyte. Record the micrometer position again at this time. The difference between the two recorded micrometer positions is the liquid film thickness measured this time. This technique can control the error range of liquid film measurements to about 5 μm.

2.2 Electrochemical measurement system

An experimental device was used to study the corrosion behaviour of zinc under external DC electric field strengths of 200 and 400 kV/m, as shown in Fig. 1. The principle of the experimental device is the same as that described in the literature [12]. A pair of stainless steel

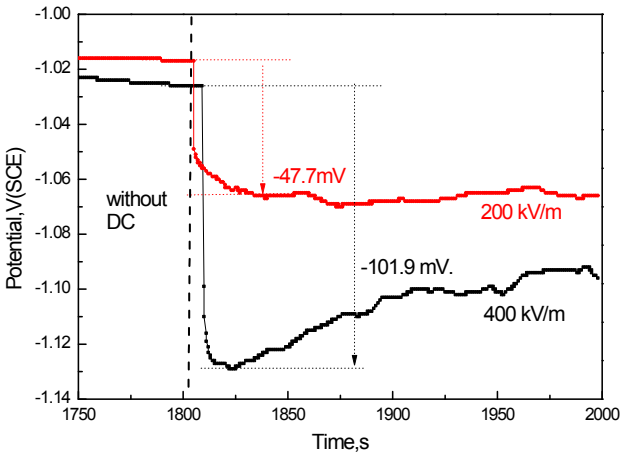

Fig. 2 Evolution of OCP for zinc covered with thin electrolyte layer (1000 μm) of 0.35% NaCl solution under external DC electric field.

plates were set opposite to each other, with a gap of 5 cm between them, as external electric field plates; one plate was grounded together with the zinc working electrode and the negative pole of a high voltage power supply (DC, LSL-BI, China), which imitated the ground mode of transmission tower, while the other plate was above working electrode and was linked to the positive pole of a high voltage power supply. A three-electrode system was applied in the electrochemical measurements. A saturated calomel electrode (SCE) was used as a reference electrode and platinum wires were used as the counter electrode. Pure zinc, as the working electrode, must be grounded, while the other test instruments were grounded virtually by using an isolation transformer.

Electrochemical measurements were performed by using a potentiostat (CHI660C, Chenhua, China). The open circuit potential (OCP) was measured as soon as the test began, and external DC electric fields were applied after the stabilization of OCP for 30min. The cathodic polarization curves of zinc under different conditions were constructed in a typical three-electrode mode after the stabilization of OCP for 30 min. The cathodic polarization curves were obtained from - 1.0 V (SCE) to - 1.6 V (SCE) versus the OCP at a scan rate of 1 mV/s. The EIS measurements under different conditions were performed at open circuit potential with a 5mV AC perturbation at the frequency from 100 kHz to 10 mHz.

All the experiments were performed at room temperature (25 ± 1 °C).

3. Results and Discussion

3.1 OCP measurements

One of the qualitative methods to study the corrosion behavior of metals is the measurements of OCP. Fig. 2 shows the evolution of the OCP for zinc covered with thin electrolyte layer (1000 μ m) of 0.35% NaCl solution under external DC electric fields.

It is found that the OCP tends to become negative after applying the external DC electric fields, which can be ascribed to the asymmetry of the zinc anode and cathode polarization [13]. Moreover, as the increasing intensity of external DC electric field, the OCP shift more negative.

3.2 Cathodic polarization measurements

Cathodic polarization was carried out to investigate the corrosion process. For zinc, the dominated cathodic reaction in corrosion process is oxygen consumption [14]. Fig. 3 shows the cathodic polarization curves of zinc covered with a 1000-μm-thick electrolyte layer under differ-

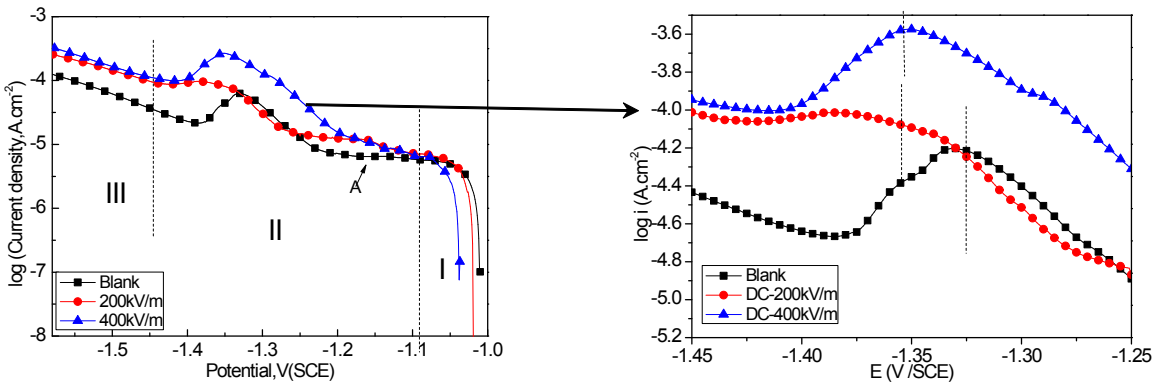

Fig. 3 Cathodic polarization curves for zinc covered with thin electrolyte layer (1000 μm) of 0.35% NaCl solution under external DC electric field (a), (b) is magnification of (a).

Table 1 Peak current density and peak potential

Environment	Covered with 1000-μm-thick electrolyte layer	
	Peak potential(V)	Peak current density (μA/cm^2)
Blank	-1.331	62.74
200Kv/m	-1.349	80.16
400Kv/m	-1.36	247.0

ent strengths of external DC electric field. Obviously, the OCP shifts negative after applying the external DC electric fields. It can be seen that the cathodic polarization curves can be divided into three regions. Region I is linear polarization near the OCP. Followed region II is the diffusion controlling range for oxygen reduction. When the polarization potential for zinc is more negative than - 1.4 V, Region III is the hydrogen evolution process. As can be observed from Fig. 3, the hydrogen evolution potential for zinc covered with a 1000-μm-thick electrolyte layer is more negative after applying the external DC electric power, which is ascribed to the increasing of pH value caused by the reduction of oxygen.

In region II (the oxygen diffusion controlling range), A is also the reduction potential range of the corrosion products [15,16].

Table 1 is the peak current density and peak potential of cathodic polarization curves shown in Fig. 3b. Obviously, after applying the external DC electric field, the peak potential of zinc covered with TEL shifts negative, and peak current density increases. Additionally, the peak potential is more negative and the peak current density is larger under the 400 kV/m DC electric field. The current peak near - 1.35 V is due to the reduction of O_2 which is the cathodic depolarizer.

Oxygen is a non-polar molecule. Water is a polar solvent. When the oxygen dissolves into water, hydrated oxygen molecules will form in the water as showed in Fig. 4.

$$O_2 + H_2O \rightarrow O_2 \cdot H_2O \quad (1)$$

$$O_2 + 2H_2O \rightarrow O_2 \cdot 2H_2O \quad (2)$$

A few research groups have studied the change of electric double layer under the low-frequency electric field [17,18], supposed that the change of the double layer was caused by the polarization of particles of the double layer, which means that the double layer model is comparable to the electric polarization model [19]. The application of an external DC electric field causes the movement of the particles of the double layers, towards the electrode having a charge opposite to that of the mobile ions in the double layer [20].Therefore, under application of an external DC electric field, the hydration oxygen molecules in the double layer can be polarized, and accelerated towards the electrode having a charge opposite to that of the mobile ions in the double layer. Consequently, the electrochemical activity of zinc increases.

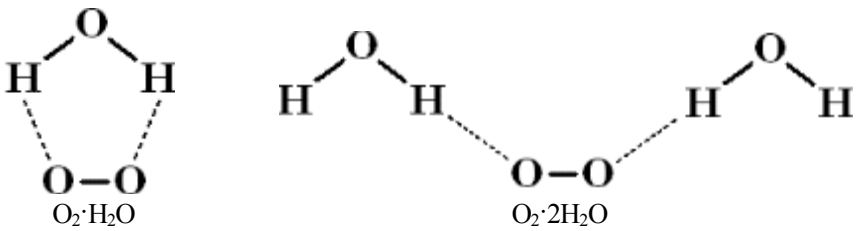

Fig. 4 Two processes of oxygen dissolution in water.

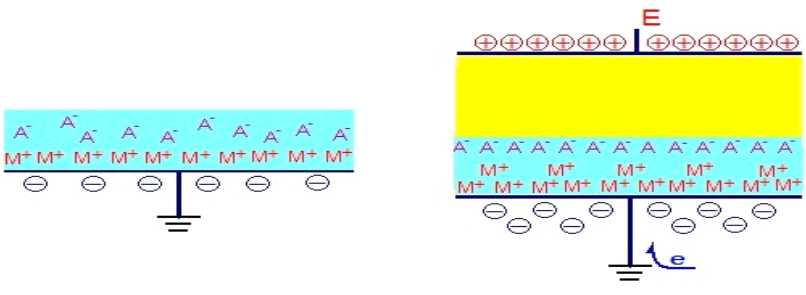

Fig. 5 Depiction of the double layer: (a) without DC electric field and (b) with DC electric field.

Compared with previous study [11], in this work, the zinc electrodes are grounded to simulate the power transmission tower; thus, the negative charges can be concentrated on the surface of the grounded electrode, resulting in the concentration of cations on the electrolyte side, including the amount of H^+ transfer to the interface of the electrode/electrolyte. Consequently, the structure of the double-layer in the electrode/electrolyte interface should be changed, and the electrode potential shift negative, as shown in Fig. 5.

In the application of the external DC electric field, the electric fields between the two stainless steels plate can be seen as the series between electric field in the air and electric field in TELs. According to electricity theory, the electric intensity (E_{out}) in TELs can be calculated by equation (3) [21].

$$E_{out} = \frac{U}{\varepsilon_r d + (1 - \varepsilon_r)t} \quad (3)$$

where U is the voltage applied to the stainless steels, ε_r is the dielectric constant, d is the distance between the two stainless steels plates; and *t* is the thickness of TELs. In the study, ε_r, d and t are all constant and therefore, E_{out} is in proportion to E_{extra}. Therefore, with increasing intensity of the external DC electric field, E_{out} become greater, and the OCP shifts more negative, this is favored for the cathodic reduction of dissolved oxygen [22].

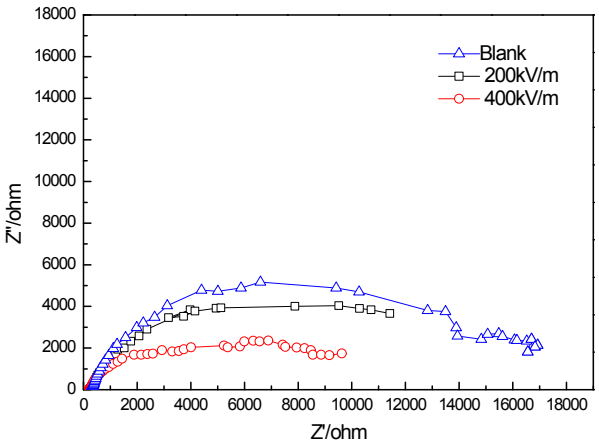

Fig. 6 Nyquist diagrams of zinc covered with TEL (1000 μm) of 0.35% NaCl solution under different conditions.

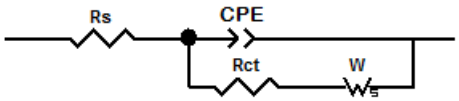

Fig. 7 Equivalent circuit for EIS fitting of Zinc.

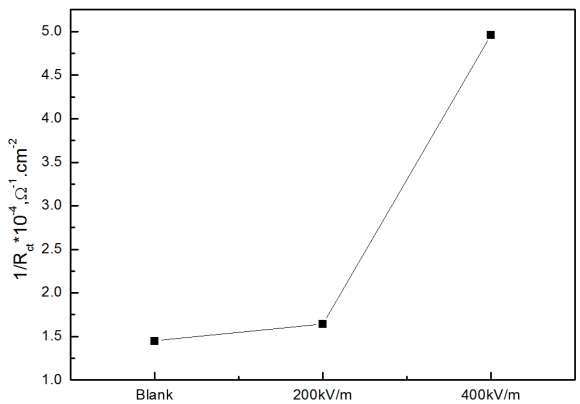

Fig. 8 Fitting results for Nyquist diagrams of zinc under different conditions.

3.3 EIS measurements

Fig. 6 shows the Nyquist diagrams of zinc covered with TEL (1000 μm) of 0.35 wt% NaCl solution under different conditions. It is seen that all Nyquist diagrams exhibit a capacitive semicircle at the high frequency and low frequency. It can be seen that the diameter of semicircle decreases gradually with increasing DC electric field, suggesting that the external electric filed could facilitate the corrosion of zinc.

Based on the above, Fig. 7 is Equivalent circuit for EIS fitting of Zinc covered with TEL (1000 μm) of 0.35 wt% NaCl solution under different conditions. Where R_s is the solution resistance; CPE is constant phase angle element; R_{ct} is the charge transfer resistance; W is the Warburg diffusion impedance.

In this study, the reciprocal of the R_{ct} was taken as a parameter to characterize the corrosion rate [13], and the values of R_{ct} for zinc covered with TEL (1000 μm) of 0.35 wt% NaCl solution under different conditions are calculated from Zsimpwin, which is a kind of software that can fit the EIS data. Fig. 8 is the fitting results for Nyquist diagrams of zinc under different conditions. It is shown that the corrosion rate of zinc covered with TEL (1000 μm) of 0.35 wt% NaCl solution without DC electric field is the smallest; and the corrosion rate of zinc under DC electric field increases and becomes the largest at the electric field of 400 kV/m.

4. Conclusions

The atmospheric corrosion behaviour of Zinc covered with TEL (1000 μm) of 0.35 wt% NaCl solution without and with different DC electric field was investigated by

open circuit potential measurements, cathodic polarization and EIS. Results indicate that the corrosion potential of zinc negatively shifts with applying of DC electric field. The applying of external DC electric field can accelerate the corrosion rate of zinc, and the zinc corrosion rate increases with increased DC electric field intensity.

However, the influence mechanism of electric field on the atmospheric corrosion of zinc is not clear, it remains to be further studied.

Acknowledgments

The authors acknowledge the financial support of Key Project of Shanghai Education Committee (No. 12ZZ170) and National Natural Science Foundation of China (No. 51271110).

References

1. D. T. Chin and T. W. Fu, *Corrosion*, **35**, 514 (1979).
2. J. L. Wendt and D. T. Chin, *Corros. Sci.*, **25**, 901 (1985).
3. R. Radeka, D. Zorovic, and D. Barisin, *Anti-Corros. Method. M.*, **27**, 13 (1980).
4. D. K. Kim, S. Muralidharan, T. H. Ha, J. H. Bae, Y. C. Ha, H. G. Lee, and J. D. Scantlebury, *Electrochim. Acta*, **51**, 5259 (2006).
5. S. Muralidharan, D. K. Kim, T. H. Ha, J. H. Bae, Y. C. Ha, H. G. Lee, and J. D. Scantlebury, *Desalination*, **216**, 103 (2007).
6. S. Goidanich, L. Lazzari, and M. Ormellese, *Corros. Sci.*, **52**, 491 (2010).
7. R. W. Bosch, and W. F. Bogaerts, *Corros. Sci.*, **40**, 323 (1998).
8. C. M. Movley, *Proc. Corrosion 2005 Conf.,* pp. 1 - 8, Houston, Texas, NACE (2005).
9. A. P. Yadav, A. Nishikata, and T. Tsuru, *Corros. Sci.*, **46**, 169 (2004).
10. V. Barranco. S. Feliu Jr, and S. Feliu, *Corros. Sci.*, **46**, 2221 (2004).
11. H. L. Huang, X. P. Guo, and Z. H. Dong, *Corros. Sci.*, **53**, 1700 (2011).
12. Y. L. Cheng, F. H. Cao, J. F. Li, J. Q. Zhang, J. M. Wang, and C. N. Cao, *Corros. Sci.*, **46**, 1649 (2004).
13. H. L. Huang, Z. Q. Pan, X. P. Guo, and Y. B. Qiu, *Corros. Sci.*, **75**, 100 (2013).
14. T. H. Muster and I. S. Cole, *Corros. Sci.*, **46**, 2319 (2004).
15. B. Zhang, H. B. Zhou, E. H. Han, and K. Wei, *Electrochim. Acta*, **54**, 6598 (2009).
16. A.P. Yadav, A. Nishikata, and T. Tsuru, J. *Electroanal. Chem.*, **585**, 142 (2005).
17. D. L. Klass, *J. Appl. Phys.*, **38**, 67 (1967).
18. D. L. Klass, *J. Appl. Phys.*, **38**, 75 (1967).
19. H. Block and J. P. Kelly, *J. Phys.* D: *Appl. Phys.*, **21**, 1661 (1988).
20. T. C. Jordan, *IEEE T. Electr. Insul.*, **24**, 849 (1989).
21. D. Y. Gao, *Yuxi Col. J.*, **8**, 82 (1986).
22. A. Panchenko, M. T. M. Koper, T. E. Shubina, S. J. Mitchell, and E. Roduner, *J. Electrochem. Soc.*, **151**, A2016 (2004).